Since January 2020 Elsevier has created a COVID-19 resource centre with free information in English and Mandarin on the novel coronavirus COVID-19. The COVID-19 resource centre is hosted on Elsevier Connect, the company's public news and information website.

Cell Stem Cell

Brief Report

Direct Exposure to SARS-CoV-2 and Cigarette Smoke Increases Infection Severity and Alters the Stem Cell-Derived Airway Repair Response

Graphical Abstract

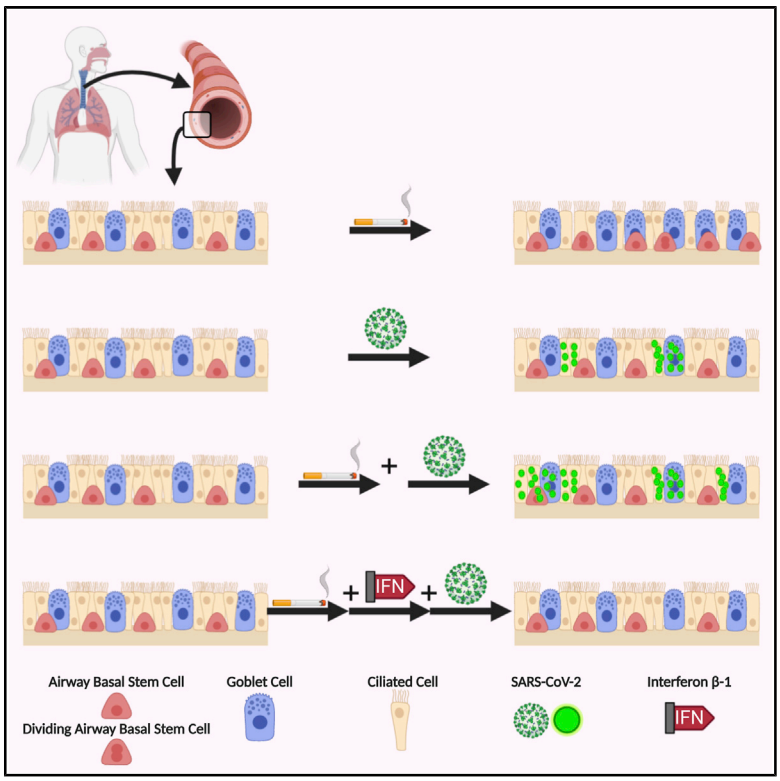

Highlights

- Direct cigarette smoke exposure increases the number of SARS-CoV-2 infected cells
- SARS-CoV-2 infection inhibits the airway basal stem cell repair response
- Cigarette smoke reduces innate immune responses with worse SARS-CoV-2 infection

Authors

Arunima Purkayastha, Chandani Sen, Gustavo Garcia, Jr., ..., Kathrin Plath, Vaithilingaraja Arumugaswami, Brigitte N. Gomperts

Correspondence

kplath@mednet.ucla.edu (K.P.), varumugaswami@mednet.ucla.edu (V.A.), bgomperts@mednet.ucla.edu (B.N.G.)

In Brief

Purkayastha and colleagues modeled the direct effects of cigarette smoke on SARS-CoV-2 infection of the airway epithelium. Acute cigarette smoke exposure increased the number of infected and apoptotic cells, prevented the normal airway basal stem cell repair response, and blunted innate immune responses. Improving innate immunity impaired SARS-CoV-2 infection.

Purkayastha et al., 2020, Cell Stem Cell *27*, 869–875
December 3, 2020
https://doi.org/10.1016/j.stem.2020.11.010

CellPress

Cell Stem Cell

CellPress

Brief Report

Direct Exposure to SARS-CoV-2 and Cigarette Smoke Increases Infection Severity and Alters the Stem Cell-Derived Airway Repair Response

Arunima Purkayastha,[1,11] Chandani Sen,[1,11] Gustavo Garcia, Jr.,[2,11] Justin Langerman,[3,11] David W. Shia,[1,4,5] Luisa K. Meneses,[1] Preethi Vijayaraj,[1] Abdo Durra,[1] Caroline R. Koloff,[1] Delilah R. Freund,[1] Justin Chi,[1] Tammy M. Rickabaugh,[1] Apoorva Mulay,[6] Bindu Konda,[6] Myung S. Sim,[7] Barry R. Stripp,[6] Kathrin Plath,[3,5,8,9,12,*] Vaithilingaraja Arumugaswami,[2,8,12,*] and Brigitte N. Gomperts[1,5,8,9,10,12,13,*]

[1]UCLA Children's Discovery and Innovation Institute, Mattel Children's Hospital UCLA, Department of Pediatrics, David Geffen School of Medicine, UCLA, Los Angeles, CA, 90095, USA

[2]Department of Molecular and Medical Pharmacology, UCLA, Los Angeles, CA 90095, USA

[3]Department of Biological Chemistry, David Geffen School of Medicine at UCLA, UCLA, Los Angeles, CA, USA

[4]UCLA Medical Scientist Training Program, David Geffen School of Medicine, UCLA, Los Angeles, CA, 90095, USA

[5]Molecular Biology Institute, UCLA, Los Angeles, CA, 90095, USA

[6]Lung and Regenerative Medicine Institutes, Cedars-Sinai Medical Center, Los Angeles, CA, USA

[7]UCLA Department of Medicine, Statistics Core, UCLA, Los Angeles, CA, USA

[8]Jonsson Comprehensive Cancer Center, UCLA, Los Angeles, CA 90095, USA

[9]Eli and Edythe Broad Stem Cell Research Center, UCLA, Los Angeles, CA 90095, USA

[10]Division of Pulmonary and Critical Care Medicine, Department of Medicine, David Geffen School of Medicine, UCLA, Los Angeles, CA 90095, USA

[11]These authors contributed equally

[12]Senior author

[13]Lead Contact

*Correspondence: kplath@mednet.ucla.edu (K.P.), varumugaswami@mednet.ucla.edu (V.A.), bgomperts@mednet.ucla.edu (B.N.G.)

https://doi.org/10.1016/j.stem.2020.11.010

SUMMARY

Current smoking is associated with increased risk of severe COVID-19, but it is not clear how cigarette smoke (CS) exposure affects SARS-CoV-2 airway cell infection. We directly exposed air-liquid interface (ALI) cultures derived from primary human nonsmoker airway basal stem cells (ABSCs) to short term CS and then infected them with SARS-CoV-2. We found an increase in the number of infected airway cells after CS exposure with a lack of ABSC proliferation. Single-cell profiling of the cultures showed that the normal interferon response was reduced after CS exposure with infection. Treatment of CS-exposed ALI cultures with interferon β-1 abrogated the viral infection, suggesting one potential mechanism for more severe viral infection. Our data show that acute CS exposure allows for more severe airway epithelial disease from SARS-CoV-2 by reducing the innate immune response and ABSC proliferation and has implications for disease spread and severity in people exposed to CS.

INTRODUCTION

Coronavirus disease (COVID-19) is an infectious disease caused by the newly discovered severe acute respiratory syndrome-related coronavirus 2 (SARS-CoV-2) and is responsible for the current pandemic that is endangering lives globally. SARS-CoV-2 is an enveloped positive-sense single-stranded RNA virus that enters its host cell by binding to the angiotensin converting enzyme 2 (ACE2) receptor (Ziegler et al., 2020). SARS-CoV-2 primarily targets the respiratory tract, and ACE2 is expressed in a gradient along the airways and is present on ciliated cells and some secretory cell subtypes (Hou et al., 2020). Severe COVID-19 lung disease has been most closely associated with older age, especially age over 65 years. Among these older hospitalized adults, underlying medical conditions have been associated with severe COVID-19, which include hypertension, obesity, diabetes mellitus, and chronic lung disease (Sanyaolu et al., 2020).

The Surgeon General's Report in 1964 determined that cigarette smoke (CS) is the most important cause of chronic lung disease, including chronic bronchitis and emphysema, in addition to causing lung cancer (U.S. Department for Health and Human Services, 2014). Mechanistically, CS has been shown to reduce mucosal innate immunity, leading to increased viral replication. The underlying mechanisms include degradation of the Type I interferon receptor (HuangFu et al., 2008), inhibition of type II interferon-dependent gene expression through a decrease in Stat1 phosphorylation (El-Mahdy et al., 2009), and reduction in

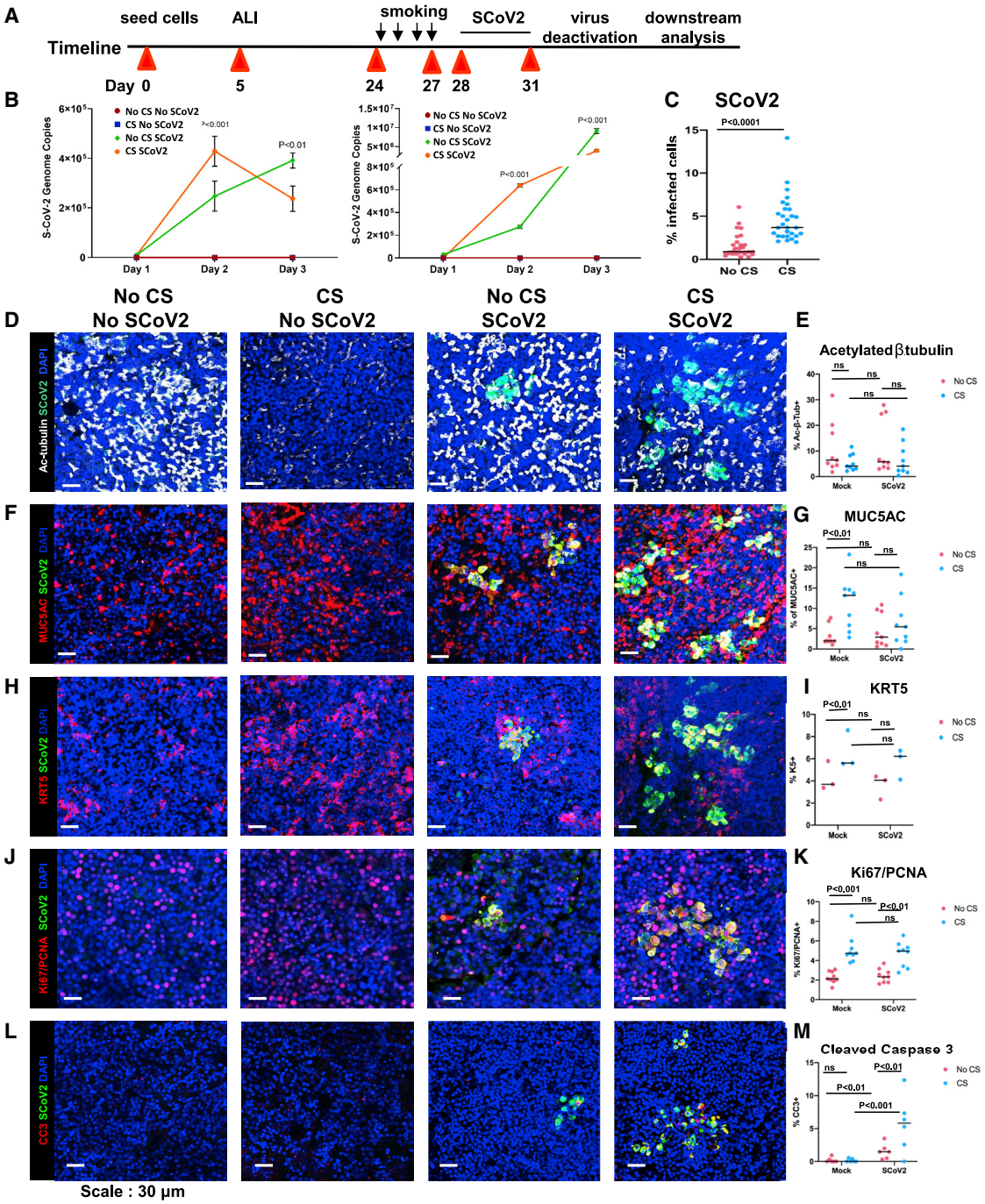

Figure 1. Cigarette Smoke Exposure Increases SARS-CoV-2 Infection in the Airway Epithelium

(A) Experimental schematic outline showing the total days in culture with days of experimental manipulations.

(B) Quantification of viral load by harvesting cells from ALI cultures with and without smoking exposure and extracting mRNA for quantitative real-time PCR of SARS-CoV-2 mRNA at 1, 2, or 3 days post infection. Data shown are from ALI cultures from two different patients. P values are calculated from technical replicates using Student's t test.

(C) Quantification of SARS-CoV-2 infected cells in ALI cultures across the four exposure conditions by IF for the SARS-CoV-2 Spike protein.

(D) IF images of ciliated cells (white) and SARS-CoV-2 (green) infected cells in ALI cultures across the four exposure conditions of no smoking and no virus, smoking and no virus, no smoking and virus, and both smoking and virus exposures.

(E) Quantification of number of ciliated cells across the four exposure groups.

(F) IF images of Muc5AC (red) mucus cells and SARS-CoV-2 (green) infected cells in ALI cultures across the four exposure conditions.

(G) Quantification of number of Muc5AC+ mucus cells across the four exposure groups.

(H) IF images of KRT5 (red) ABSCs and SARS-CoV-2 (green) in ALI cultures across the four exposure conditions.

(legend continued on next page)

the immediate-early, inductive, and amplification phases of the type I IFN response that were abrogated with glutathione antioxidant treatment (Bauer et al., 2008).

Given the importance of CS in the development of chronic lung diseases, it has been suggested that CS may be a significant risk factor for severe COVID-19. The World Health Organization concluded that CS is associated with increased severity of disease and death in hospitalized COVID-19 patients, although they could not quantify the risk to smokers (Igić, 2020). The lack of clarity on the issue is likely because there has been a lower than expected prevalence of CS reported in retrospective and observational databases because of incomplete reporting of smoking status in patients in emergency situations. Therefore, some studies reported no increase in CS-related disease whereas more in depth analyses of demographic data showed an increased risk of severe COVID-19 associated with CS (Guo, 2020, Vardavas and Nikitara, 2020, Zhao et al., 2020). In addition, a recent study showed that CS is a risk factor for more severe COVID-19 among young adults (Adams et al., 2020). Several studies have examined ACE2 expression in the airways of smokers and found that CS increases ACE2 expression (Zhang et al., 2020, Cai et al., 2020). However, there have been no direct studies to examine the effect of CS on the airway epithelium in the setting of SARS-CoV-2 infection, and therefore it has remained unclear as to whether CS influences SARS-CoV-2 infection.

Therefore, we developed a system to expose primary human mucociliary epithelial cultures at the air-liquid interface (ALI) to CS and subsequently infected the cultures with SARS-CoV-2. CS exposure of the ALI cultures has been shown to mimic the *in vivo* acute CS exposure seen in patients (Gindele et al., 2020). We found an increase in the number of infected cells after CS exposure and that acute CS exposure increases airway basal stem cells (ABSCs) while SARS-CoV-2 infection prevents the normal repair response from ABSCs. We also found that SARS-CoV-2 infection upregulates the interferon response, while short-term CS exposure reduces the interferon response, suggesting that the modulation of the interferon response by SARS-CoV-2 is causally linked to more active infection in CS-exposed cultures. Consistent with this hypothesis, we found that the CS-induced increase in SARS-CoV-2 infection could be abrogated by treatment with exogenous interferon β-1.

RESULTS

Cigarette Smoke Exposure Increases SARS-CoV-2 Infection in the Airway Epithelium, and SARS-CoV-2 Prevents the Stem Cell-Mediated Repair Response

We used primary human ABSCs from three different healthy lung transplant donors and two other nonsmoker donors from commercial sources for ALI cultures (Gruenert et al., 1995). The cultures were exposed to or mock exposed to short-term CS for 4 days and then infected or mock infected with SARS-CoV-2 at a multiplicity of infection (MOI) of 0.1 (Figure 1A). At one, two, and three days after infection or mock treatment, we examined the cultures for evidence of SARS-CoV-2 replication. We performed quantitative real-time PCR on RNA obtained from the airway epithelial cells at these time points and performed this time course on two biological replicates. We consistently found that the highest intracellular viral genome copies (based on N gene transcripts) was at 48 h post infection and that there was a 2- to 3-fold increase in viral load in samples that were first exposed to CS (Figure 1B). This is consistent with the fold increase in the number of infected cells seen by immunofluorescence (IF) staining for SARS-Co-V-2 Spike protein at 72 h post infection (Figure 1C). However, at 72 h post infection, we saw variability in viral genome copies in CS exposed cultures (Figure 1B), and this is consistent with the cells with the highest viral load becoming apoptotic and being extruded from the cultures and may also reflect the complexity of the genetic backgrounds of the different patients. Infectious virions released to the basal chamber culture media were below detectable levels at these time points. We found an increased number of infected cells in ALI cultures that had CS exposure, which was consistent across 5 patient samples and 25 technical replicates from these 5 patients ($p < 0.0001$) (Figure 1C).

Next, we quantified the number of ciliated and secretory airway epithelial cell types across all conditions by IF for cell-type-specific markers (Figures 1D–1G). We found that CS exposure alone showed a trend toward a decrease in the number of ciliated cells ($p = 0.06$) marked by the presence of acetylated β-tubulin and significantly increased the number of Muc5AC-expressing mucus cells ($p < 0.001$) (Figures 1D–1G). We found that the number of ciliated or mucus cells did not significantly change with SARS-CoV-2 infection (Figures 1D–1G). We then assessed the number of ABSCs, the key stem cell type orchestrating the repair response by proliferation, by IF for keratin 5 (KRT5). We found that CS significantly increased the number of ABSCs as part of a repair response ($p < 0.01$) and that SARS-CoV-2 viral infection alone or viral infection with CS did not trigger the expected increase in ABSCs needed for repair (Figures 1H and 1I). The repair response is mediated by proliferation of ABSCs as well as transient amplifying cells in the ALI cultures. We therefore assessed all proliferating cells in the ALI cultures by immunostaining for Ki67 combined with PCNA. We found that proliferation was induced after CS exposure but that SARS-CoV-2 infection did not further alter the proliferation under the CS and control conditions, implying that SARS-CoV-2 inhibits the repair process in the airway epithelium (Figures 1J and 1K). IF for

(I) Quantification of number of ABSCs across the four exposure groups.
(J) IF images of both Ki67 and PCNA (red) and SARS-CoV-2 (green)-expressing cells in ALI cultures across the four exposure conditions.
(K) Quantification of number of proliferating cells across the four exposure groups.
(L) IF images of cleaved caspase 3 (CC3)(white) and SARS-CoV-2 (green) for apoptosis across the four exposure conditions.
(M) Quantification of number of apoptotic cells across the four exposure groups.
Graph represents mean ± SEM, n = 5 biological replicates (5 different patients), each with 3–5 technical replicates (3–5 ALI transwell cultures derived from each of the 5 different patients) except for KRT5 and CC3 IF with quantification from 2 biological replicates (2 different patients), each with 3 technical replicates (3 ALI transwell cultures derived from each of the 2 different patients). Each dot represents a technical replicate. P values are calculated from all technical replicates across the biological replicates as described above. ns, not significant by Student's t test. Scale bar, 30 μm.

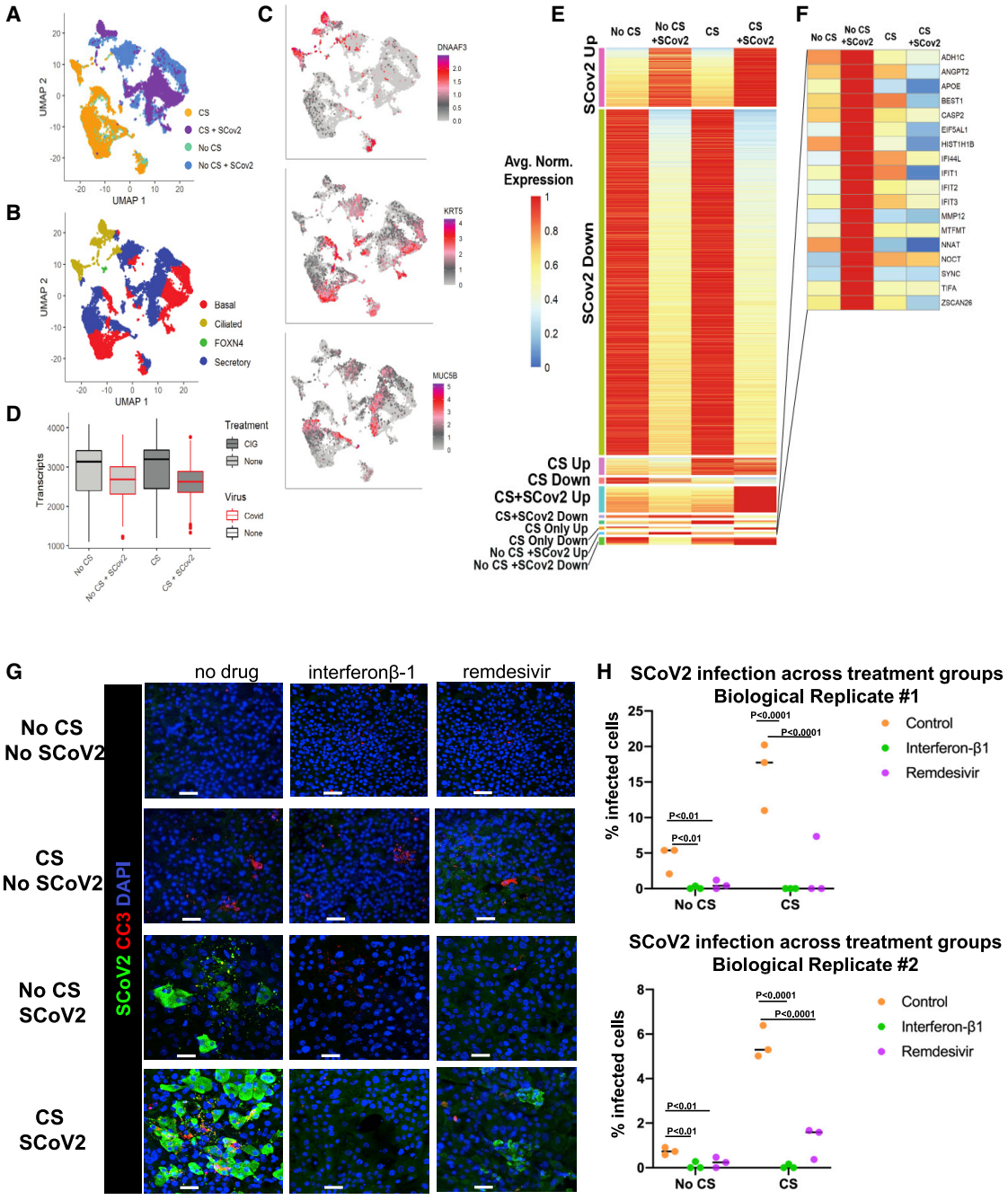

Figure 2. Smoking Reduces the Interferon Response in SARS-CoV-2 Infection, and Interferon Abrogates Infection after Cigarette Smoke Exposure

(A) Reduced dimensionality graph showing the position of 19,361 cells exposed to no cigarette smoke or virus, cigarette smoke (CS) alone or virus (SARS-CoV-2) alone, or cigarette smoke and virus. Cells are identified as shown in the key.

(B) On the same plot as in (A), cell types are shown based on the expression of known human airway genes. Cell type is colored as shown in the key.

(C) Shown are cells colored by their normalized expression value of cell type marker genes *Dnaaf3* (ciliated cells), *Krt5* (basal cells), and *Muc5b* (secretory cells).

(D) Boxplots which capture the distribution of normalized transcripts in all cells per sample, as separated by cigarette smoke and SARS-CoV-2 exposure.

(E) Heatmap showing the percent expression of all genes found to be differentially expressed in at least one condition. CS indicated cigarette smoke treatment and SCov2 indicates SARS-CoV-2 viral exposure.

(F) Popout of heatmap showing the specific genes which are induced by SARS-CoV-2 but not in cigarette smoke exposure with SARS-CoV-2 (No CS + SCov2 Up).

(G) IF images of SARS-CoV-2 (green) infected cells across the four exposure groups with no drug treatment, interferon β-1, or remdesivir treatment.

(legend continued on next page)

cleaved caspase 3 (CC3), across two biological replicates and six technical replicates at 3 days post infection, revealed that apoptosis was infrequently seen in the ALI cultures with CS exposure alone, but viral infection significantly increased the number of apoptotic cells, and the combination of CS and infection further increased the number of apoptotic cells (Figures 1L and 1M). Based on these data, SARS-CoV-2 infection is promoting cell death while reducing the normal airway epithelial repair response. As ACE2 is the receptor for SARS-CoV-2, we examined ACE2 expression by IF and found that there was a trend toward increased ACE2 expression after CS exposure and that there was no change in ACE2 expression in infected cells or infected cells exposed to CS (Lee et al., 2020) (Figures S1A and S1B). Quantitative real-time PCR revealed no change in ACE2 gene expression across all exposure groups and across our infection time course (Figure S1C). Overall, across five different patients, we found a significant increase in the number of SARS-CoV-2 infected cells after CS exposure and differences in cellular responses to these airway exposures.

Smoking Reduces the Innate Immune Response in SARS-CoV-2 Infection, and Interferon Treatment Abrogates Infection after Cigarette Smoke Exposure

We then sought to determine a possible mechanism for the more active cellular infection seen upon exposure of the ALI cultures to both CS and SARS-CoV-2. We applied single-cell RNA-sequencing to determine the transcriptional alterations taking place which might explain the differences in SARS-CoV-2 infectivity between CS exposure and no exposure. We used the same experimental timeline as outlined in the schematic in Figure 1A before performing single-cell dissociation for RNA-seq. We recovered 19,361 single-cell transcriptomes that passed filtration criteria. Plotting of the data showed that mock-treated cells and cells exposed to CS were largely mixed and that cells with SARS-CoV-2 infection were separated (Figure 2A), indicating that SARS-CoV-2 infection induced profound transcriptional changes at the time point examined. Despite these differences, we detected all major expected cell types of the lung epithelium within the ALI cultures (Figure 2B), expressing typical human airway cell type marker genes (DNAAF3, ciliated cells; KRT5, basal cells; and SCGB1A1 and MUC5B, secretory cells; Figure 2C; Figure S2C). We detected SARS-CoV-2 transcripts in all major cell types and found the proportion of infected cells to be highest in FOXN4+ cells (Figure S2A); however, very few FOXN4+ cells were detected (Figure 2A).

We observed a global downregulation of genes in SARS-CoV-2 exposed samples, with approximately 10%–15% fewer transcripts in infected cells compared to uninfected controls (Figure 2D). Both CS-exposed and unexposed samples yielded this pattern, suggesting that it is not a unique handling of the sample. Future studies are required to explore the mechanisms leading to this observation. Using differential expression to determine genes specific to each condition, we detected the downregulation of 2,805 genes in SARS-CoV-2 exposed samples, which was consistent across all major cell types (Figure 2E; Figure S2B). Among the downregulated genes were genes related to the viral immune response and various metabolic processes. 475 genes were upregulated upon exposure to the virus, including genes related to interferon signaling and chromatin organization. Although the majority of gene expression changes were controlled by virus exposure, we found another 559 genes that were altered in response to CS exposure. Even prior to virus exposure, CS downregulated the innate immune response and stimulated airway differentiation genes. In response to SARS-CoV-2, CS-treated cells downregulated genes related to metabolic and wound healing processes and upregulated cilia-related genes. Interestingly, a small class of genes was induced in the non-CS-exposed cells in response to SARS-CoV-2 but downregulated in the CS-exposed infected ALI cultures. These genes included interferon-induced protein with tetratricopeptide repeats (IFIT) *IFIT1*, *IFIT2*, *IFIT3*, and interferon-induced protein 44-like (*IFI44L)* and indicated an interferon mediated response induced by viral infection that was repressed below the level in control cells in infected CS-treated cells (Figure 2F; Table S3). Together these data suggest that CS exposure prevents an effective interferon-based response to the SARS-CoV-2 virus.

Because the interferon response was increased in viral infection alone but decreased in the setting of CS with viral infection, we reasoned that the greater infection seen upon treatment with CS and SARS-CoV-2 was, at least in part, due to CS-induced reduction in the innate immune response. We therefore treated the CS-exposed or unexposed and virally infected or uninfected ALI cultures with interferonβ-1 and included remdesivir (a direct acting antiviral agent) or no drug, as controls. These were added to the ALI cultures after CS exposure and just prior to viral infection and were present in the cultures for three days after which the cultures were immunostained for the apoptotic marker CC3 and Spike antigen. We found that interferon β-1 completely abrogated the infection (Figures 2G and 2H). Remdesivir also showed an inhibitory response to viral infection, and these effects were most pronounced in the ALI cultures that received CS-exposure prior to infection (Figure 2H). This shows that a lack of interferon response is at least one important mechanism for the higher SARS-CoV-2 infectivity seen in CS exposed ALI cultures.

DISCUSSION

There has been some controversy about whether CS exposure increases SARS-CoV-2 infectivity and whether this might lead to more severe disease. Our primary human mucociliary epithelial cell culture model with direct exposure to CS and SARS-CoV-2 infection demonstrates that short-term exposure to CS in primary human airway cells from previously healthy patients who were not chronic smokers leads to increased infection. Our data suggest two potential and synergistic mechanisms for this: reduced innate immunity of the cells leading to more active infection and lack of ABSCs to appropriately proliferate for airway repair after infection, which could lead to worse tissue

(H) Quantification of the number of infected cells with each treatment in the four exposure groups. Two biological replicates are shown.
Graph represents mean, n = 2 biological replicates (2 different patients), each with 3 technical replicates (3 different ALI transwell cultures derived from each of the 2 patients for all three treatment groups and four environmental exposure conditions). Each dot represents a technical replicate. P values are calculated from technical replicates across each of the biological replicates described above. ns, not significant by Student's t test. Scale bar, 50 μm.

damage and/or stem cell exhaustion and increased apoptosis in airway cells exposed to CS and SARS-CoV-2.

The reduction in the interferon response by smoking is one mechanism whereby SARS-CoV-2 may more easily enter and replicate in epithelial cells. Interestingly, interferon response genes were actually induced by the virus, which may explain why we only see a low percentage of infected cells in the ALI cultures and why the majority of the human population does not develop severe respiratory infections. Our data suggest that there are additional factors from CS exposure that could make the cells more vulnerable to infection. For example, the synergistic increase in apoptotic cells after CS exposure and infection suggests that the CS may act with the virus to potentiate other pathways, such as the DNA damage response pathway, to injure the epithelium. We also saw a reduction in cell division in the ABSCs which prevented the normal host response with repair and regeneration of the airway. This result was in contrast to smoking injury where ABSCs proliferate robustly to repair the airway epithelium. Despite smoking injury, the SARS-CoV-2 response was dominant and prevented the normal ABSC proliferation response.

The interferon response is reported to be reduced or delayed in serum levels in ferrets and patients with severe COVID-19 where pro-inflammatory cytokines and chemokines are more dominant (Blanco-Melo et al., 2020). Others have found a temporal expression of interferon genes after SARS-CoV-2 infection (Yoshikawa et al., 2010). We noted an increase in interferon response genes in ALI cultures at 3 days post infection with low MOI (0.1). This suggests that an intact, normal airway epithelium could function as a barrier to COVID-19 with an innate immune response and could explain why the majority of infected individuals have mild symptoms and even asymptomatic carriage. Abrogation of SARS-CoV-2 infection with type I interferons has been reported by others in other settings (Lokugamage et al., 2020; Mantlo et al., 2020), including a small clinical trial (Wang et al., 2020).

The human primary ALI cell culture model provides a useful system for studying the direct effects of CS on the airway epithelium. Our experiments directly examined the effects of short-term CS exposure on the airway, which implies that current smokers are at risk of more severe infection. It is not clear whether former smokers will have the same risk of infection that current smokers do, and this is something that remains to be tested. Our acute CS exposure of ALI cultures did not show increased ACE2 expression, as has been previously demonstrated, but likely reflects the short time frame of exposure and the low expression of ACE2 in the distal trachea. The increased number of infected cells in smokers has implications for more severe infection in smokers resulting in increased lung disease, although our cultures are of the proximal airways so we could not directly assess for effects on diffuse alveolar damage or acute respiratory distress syndrome (ARDS). Overall, our data provide evidence for the need for health measures to stop smoking to reduce severe COVID-19.

Limitations of Study

There are several factors that make these studies challenging. The first is that there is a wide variation in the differentiation capacity of the ALI cultures from different donors, together with variation in the number of SARS-CoV-2 infected cells in each set of cultures. Therefore, it can be challenging to assess effects across heterogeneous patient samples. In addition, the sample size is limited by the challenges and costs of obtaining human tissue. This limits the number of patient samples and number of replicates that can be performed from each patient. There are also many changes that occur in the cell after infection, and the timing of these is critical. We found that time courses were very helpful in determining the point of greatest infection and that this time point was quite consistent across cultures. However, this point of maximal viral load didn't necessarily correspond with the biggest changes in cell types or apoptosis. One other limitation of our model is the lack of inflammatory cells, and this is something that we are currently incorporating into our models.

STAR★METHODS

Detailed methods are provided in the online version of this paper and include the following:

- KEY RESOURCES TABLE
- RESOURCE AVAILABILITY
  - Lead Contact
  - Materials Availability
  - Data and Code Availability
- EXPERIMENTAL MODELS AND SUBJECT DETAILS
  - Human Tissue Procurement
  - ABSC Isolation
  - Air-Liquid Interface Cultures
  - Tracheal Epithelial Cell Plus and Serum-Free Media
  - Cigarette Smoke *In Vitro* Treatments
  - SARS-CoV-2 infection
  - Interferonβ-1 Drug Study
- METHOD DETAILS
  - Immunocytochemistry, Confocal Imaging and Cell Counting
  - Quantitative Polymerase Chain Reaction
  - Viral Titer Measurement
  - Single Cell Library Generation and Sequencing
  - Sequencing Data Analysis
- QUANTIFICATION AND STATISTICAL ANALYSIS

SUPPLEMENTAL INFORMATION

Supplemental Information can be found online at https://doi.org/10.1016/j.stem.2020.11.010.

ACKNOWLEDGMENTS

We would like to thank Andrew Lund and WooSuk Choi for their input on the manuscript. This work was supported by the NIH/NCI Grant R01CA208303 (B.N.G.), the Tobacco-Related Disease Research Program (TRDRP) High Impact Pilot Research Award (HIPRA) 26IP-0036 (B.N.G.), the TRDRP HIPRA 29IP-0597 (B.G.), the UCOP Emergency Funding COVID19 TRDRP Seed grant Award R00RG2383 (B.N.G.), the Burroughs Wellcome Fund under the Innovation in Regulatory Science Award Program (B.N.G.), the California Institute for Regenerative Medicine DISC2COVID11764 award (B.N.G., V.A.), the Ablon Research Scholars Award (B.N.G.), the UCLA Oversight COVID-19 Research Committee (OCRC) (B.N.G., V.A.), the UCLA Eli & Edythe Broad Center of Regenerative Medicine and Stem Cell Research (BSCRC) (B.N.G.), and the UCLA Medical Scientist Training Program grant (NIH NIGMS GM008042) (D.W.S.). K.P. was supported by the UCLA BSCRC, the David Geffen School of Medicine, NIH P01 GM099134, and a Faculty Scholar grant from the Howard

Hughes Medical Institute. We appreciate the UCLA BSCRC Microscopy Core and the UCLA Translational Pathology Core Laboratory. This research was supported by NIH National Center for Advancing Translational Science (NCATS) UCLA CTSI Grant Number UL1TR001881. The following reagent was obtained through BEI Resources, NIAID, NIH: Polyclonal Anti-SARS Coronavirus (antiserum, Guinea Pig), NR-10361. The graphical abstract was created with Biorender.com.

AUTHOR CONTRIBUTIONS

A.P., C.S., G.G., J.L.: conception and design, collection and assembly of data, data analysis and interpretation. P.V., L.K.M., D.W.S., T.M.R.: data analysis and interpretation and technical support. V.A., K.P.: conception and design, data analysis and interpretation, manuscript writing. M.S.S., A.D., C.R.K., D.R.F., J.L.: data analysis and interpretation. B.R.S., A.M., B.K.: conception and design. B.N.G.: conception and design, data analysis and interpretation, manuscript writing, final approval of the manuscript and financial support.

DECLARATION OF INTERESTS

The authors declare no competing interests.

Received: July 29, 2020
Revised: October 31, 2020
Accepted: November 13, 2020
Published: November 17, 2020

REFERENCES

Adams, S.H., Park, M.J., Schaub, J.P., Brindis, C.D., and Irwin, C.E., Jr. (2020). J Adolesc Health *67*, 362–368.

Bauer, C.M.T., Dewitte-Orr, S.J., Hornby, K.R., Zavitz, C.C.J., Lichty, B.D., Stämpfli, M.R., and Mossman, K.L. (2008). Cigarette smoke suppresses type I interferon-mediated antiviral immunity in lung fibroblast and epithelial cells. J. Interferon Cytokine Res. *28*, 167–179.

Blanco-Melo, D., Nilsson-Payant, B.E., Liu, W.C., Uhl, S., Hoagland, D., Møller, R., Jordan, T.X., Oishi, K., Panis, M., Sachs, D., et al. (2020). Imbalanced Host Response to SARS-CoV-2 Drives Development of COVID-19. Cell *181*, 1036–1045.e9.

Cai, G., Bossé, Y., Xiao, F., Kheradmand, F., and Amos, C.I. (2020). Tobacco Smoking Increases the Lung Gene Expression of ACE2, the Receptor of SARS-CoV-2. Am. J. Respir. Crit. Care Med. *201*, 1557–1559.

El-Mahdy, S., Modestou, M., Manzel, L., and Look, D. (2009). Inhibition of Antiviral Defense in Airway Epithelial Cells by Cigarette Smoke. Proceedings of the American Thoracic Society 2009 International Conference, A3227.

Gauger, P.C., and Vincent, A.L. (2014). Serum virus neutralization assay for detection and quantitation of serum-neutralizing antibodies to influenza A virus in swine. Methods Mol. Biol. *1161*, 313–324.

Gindele, J.A., Kiechle, T., Benediktus, K., Birk, G., Brendel, M., Heinemann, F., Wohnhaas, C.T., LeBlanc, M., Zhang, H., Strulovici-Barel, Y., et al. (2020). Intermittent exposure to whole cigarette smoke alters the differentiation of primary small airway epithelial cells in the air-liquid interface culture. Sci. Rep. *10*, 6257.

Gruenert, D.C., Finkbeiner, W.E., and Widdicombe, J.H. (1995). Culture and transformation of human airway epithelial cells. Am. J. Physiol. *268*, L347–L360.

Guo, F.R. (2020). Smoking links to the severity of COVID-19: An update of a meta-analysis. J. Med. Virol. https://doi.org/10.1002/jmv.25967.

Hegab, A.E., Ha, V.L., Attiga, Y.S., Nickerson, D.W., and Gomperts, B.N. (2012a). Isolation of basal cells and submucosal gland duct cells from mouse trachea. J. Vis. Exp. (67), e3731.

Hegab, A.E., Ha, V.L., Darmawan, D.O., Gilbert, J.L., Ooi, A.T., Attiga, Y.S., Bisht, B., Nickerson, D.W., and Gomperts, B.N. (2012b). Isolation and in vitro characterization of basal and submucosal gland duct stem/progenitor cells from human proximal airways. Stem Cells Transl. Med. *1*, 719–724.

Hegab, A.E., Ha, V.L., Bisht, B., Darmawan, D.O., Ooi, A.T., Zhang, K.X., Paul, M.K., Kim, Y.S., Gilbert, J.L., Attiga, Y.S., et al. (2014). Aldehyde dehydrogenase activity enriches for proximal airway basal stem cells and promotes their proliferation. Stem Cells Dev. *23*, 664–675.

Hou, Y.J., Okuda, K., Edwards, C.E., Martinez, D.R., Asakura, T., Dinnon, K.H., 3rd, Kato, T., Lee, R.E., Yount, B.L., Mascenik, T.M., et al. (2020). Cell *182*, 429–446.

HuangFu, W.C., Liu, J., Harty, R.N., and Fuchs, S.Y.; HuangFu (2008). Cigarette smoking products suppress anti-viral effects of Type I interferon via phosphorylation-dependent downregulation of its receptor. FEBS Lett. *582*, 3206–3210.

Igić, R. (2020). Smoking and COVID-19. Vojnosanit. Pregl. *77*, 461–462.

Lee, I.T., Nakayama, T., Wu, C.-T., Goltsev, Y., Jiang, S., Gall, P.A., Liao, C.-K., Shih, L.-C., Schürch, C.M., McIlwain, D.R., et al. (2020). ACE2 localizes to the respiratory cilia and is not increased by ACE inhibitors or ARBs. Nat. Commun. *11*, 5453.

Lokugamage, K.G., Hage, A., de Vries, M., Valero-Jimenez, A.M., Schindewolf, C., Dittmann, M., Rajsbaum, R., and Menachery, V.D. (2020). Type I Interferon Susceptibility Distinguishes SARS-CoV-2 from SARS-CoV. J. Virol. *94*, e01410-20. Published online July 13, 2020.

Mantlo, E., Bukreyeva, N., Maruyama, J., Paessler, S., and Huang, C. (2020). Antiviral activities of type I interferons to SARS-CoV-2 infection. Antiviral Res. *179*, 104811.

Paul, M.K., Bisht, B., Darmawan, D.O., Chiou, R., Ha, V.L., Wallace, W.D., Chon, A.T., Hegab, A.E., Grogan, T., Elashoff, D.A., et al. (2014). Dynamic changes in intracellular ROS levels regulate airway basal stem cell homeostasis through Nrf2-dependent Notch signaling. Cell Stem Cell *15*, 199–214.

Plasschaert, L.W., Žilionis, R., Choo-Wing, R., Savova, V., Knehr, J., Roma, G., Klein, A.M., and Jaffe, A.B. (2018). A single-cell atlas of the airway epithelium reveals the CFTR-rich pulmonary ionocyte. Nature *560*, 377–381.

Sanyaolu, A., Okorie, C., Marinkovic, A., Patidar, R., Younis, K., Desai, P., Hosein, Z., Padda, I., Mangat, J., and Altaf, M. (2020). Comorbidity and its Impact on Patients with COVID-19. SN Compr Clin Med, 1–8, 10.1007/s42399-020-00363-4.

U.S. Department of Health and Human Services (2014). The Health Consequences of Smoking: 50 Years of Progress. A Report of the Surgeon General (U.S. Department of Health and Human Services, Centers for Disease Control and Prevention, National Center for Chronic Disease Prevention and Health Promotion, Office on Smoking and Health).

Vardavas, C.I., and Nikitara, K. (2020). COVID-19 and smoking: A systematic review of the evidence. Tob. Induc. Dis. *18*, 20.

Wang, N., Zhan, Y., Zhu, L., Hou, Z., Liu, F., Song, P., Qiu, F., Wang, X., Zou, X., Wan, D., et al. (2020). Retrospective Multicenter Cohort Study Shows Early Interferon Therapy Is Associated with Favorable Clinical Responses in COVID-19 Patients. Cell Host Microbe *28*, 455–464.e2.

Yoshikawa, T., Hill, T.E., Yoshikawa, N., Popov, V.L., Galindo, C.L., Garner, H.R., Peters, C.J., and Tseng, C.T. (2010). Dynamic innate immune responses of human bronchial epithelial cells to severe acute respiratory syndrome-associated coronavirus infection. PLoS ONE *5*, e8729.

Zhang, H., Rostami, M.R., Leopold, P.L., Mezey, J.G., O'Beirne, S.L., Strulovici-Barel, Y., and Crystal, R.G. (2020). Expression of the SARS-CoV-2 *ACE2* Receptor in the Human Airway Epithelium. Am. J. Respir. Crit. Care Med. *202*, 219–229.

Zhao, Q., Meng, M., Kumar, R., Wu, Y., Huang, J., Lian, N., Deng, Y., and Lin, S. (2020). The impact of COPD and smoking history on the severity of COVID-19: A systemic review and meta-analysis. J. Med. Virol., 10.1002/jmv.25889.

Zhou, Y., Zhou, B., Pache, L., Chang, M., Khodabakhshi, A.H., Tanaseichuk, O., Benner, C., and Chanda, S.K. (2019). Metascape provides a biologist-oriented resource for the analysis of systems-level datasets. Nat. Commun. *10*, 1523.

Ziegler, C.G.K., Allon, S.J., Nyquist, S.K., Mbano, I.M., Miao, V.N., Tzouanas, C.N., Cao, Y., Yousif, A.S., Bals, J., Hauser, B.M., et al.; HCA Lung Biological Network. Electronic address: lung-network@humancellatlas.org; HCA Lung Biological Network (2020). SARS-CoV-2 Receptor ACE2 Is an Interferon-Stimulated Gene in Human Airway Epithelial Cells and Is Detected in Specific Cell Subsets across Tissues. Cell *181*, 1016–1035.e19.

STAR★METHODS

KEY RESOURCES TABLE

REAGENT or RESOURCE	SOURCE	IDENTIFIER
Antibodies		
Rabbit Keratin 5	Covance	Cat # PRB-160P; RRID:AB_291581
Mouse Acetylated β-Tubulin	Sigma	Cat# T7451; RRID:AB_609894
Rabbit Acetylated α-Tubulin	Cell Signaling Technology	Cat# mAb#5335
Guinea pig Anti-SARS Coronavirus	BEI Resources, NIAID, NIH	Cat # NR-10361
Mouse Muc5AC	ThermoFisher	Cat # MA5-12178
Rabbit Ki67	R&D Biosystems	Cat#: AF7617
Mouse PCNA	Abcam	Cat# ab29
Rabbit CC3	Cell Signaling Technology	Cat#9661
Goat anti-Rabbit IgG (H+L) Highly Cross-Adsorbed Secondary Antibody, Alexa Fluor 594	ThermoFisher	Cat# A-11037; RRID:AB_2534095
Goat anti-Mouse IgG (H+L) Highly Cross-Adsorbed Secondary Antibody, Alexa Fluor 488	ThermoFisher	Cat# A-11029; RRID:AB_138404
Goat anti-Guinea Pig IgG (H+L) Cross-Adsorbed Secondary Antibody, Alexa Fluor 488	ThermoFisher	Cat# A-11073; RRID:AB_2534117
Goat anti-Mouse IgG (H+L) Highly Cross-Adsorbed Secondary Antibody, Alexa Fluor 647	ThermoFisher	Cat# A-21235
Biological Samples		
Human bronchiolar airway tissue specimens	Ronald Reagan UCLA Medical Center	N/A
Normal human bronchial epithelial cells	Lonza	N/A
Chemicals, Peptides, and Recombinant Proteins		
Dispase	Corning	Cat# 354235
Collagen type I	Corning	Cat# 354249
HEPES	Sigma	Cat# H0887
Sodium Bicarbonate	Life Technologies	Cat# 25080-094
L-glutamine	Invitrogen	Cat# 35050-061
Insulin	Sigma	Cat# I6634
Transferrin	Sigma	Cat# T5391
Cholera Toxin	Sigma	Cat# C8052
Epidermal Growth Factor (EGF)	Corning	Cat# 354001
Bovine Pituitary Extract	Invitrogen	Cat# 13028-014
Fetal Bovine Serum	ThermoFisher	Cat# SH3008803HI
Bovine Serum Albumin	ThermoFisher	Cat# BP9706
Retinoic Acid	Sigma	Cat# R2625
Recombinant Human Interferonβ-1	Peprotech	Cat# 300-02BC
Remdesivir (GS-5734)	Selleck Chemicals	Cat# S8932
Deposited Data		
Single-cell RNA seq	This paper	GEO: accession # "GEO: GSE161089"
Oligonucleotides		
Primers for viral load, see Table S3	This paper	N/A
hACE2 (Hs01085333_m1)	Thermo Fisher Scientific	Cat#4331182
Software and Algorithms		
GraphPad Prism 7	GraphPad Software	RRID:SCR_002798
Fiji	ImageJ	RRID:SCR_002285

CellPress

RESOURCE AVAILABILITY

Lead Contact

Further information and requests for resources and reagents should be directed to and will be fulfilled by the Lead Contact, Brigitte N. Gomperts.

Materials Availability

This study did not generate new unique reagents.

Data and Code Availability

This study generated a single cell RNA sequencing dataset of ALI cultures that were exposed to cigarette smoke and/or SARS-CoV-2 or neither.Original data have been deposited to Mendeley Data: https://doi.org/10.17632/jj7vb9jzk9.1.

The annotated scRNA-seq data can be browsed with an interactive web-tool, courtesy of the Chan-Zuckerberg Initiative. The raw scRNA-seq data was deposited in NCBI's GEO database. The accession number for the single cell RNA sequencing reported in this paper is GEO:GSE161089.

EXPERIMENTAL MODELS AND SUBJECT DETAILS

Human Tissue Procurement

Large airways and bronchial tissues were acquired from de-identified normal human donors after lung transplantations at the Ronald Reagan UCLA Medical Center. Tissues were procured under Institutional Review Board-approved protocols at the David Geffen School of Medicine at UCLA. For some experiments normal human bronchial epithelial cells (NHBE) from non-smokers were obtained from Lonza and all samples were de-identified. ABSCs were used from five different biological replicates and ABSCs from one biological replicate was used for two experiments. The biological replicates were from ABSCs isolated from lung transplant donors or NHBE samples from Lonza. No demographic data was available for the normal lung donor samples. Lonza samples were obtained from lungs from donors ranging from 30-50 years and represented both males and females. No significant difference was seen between the ALI cultures from cells from these two sources.

ABSC Isolation

Human ABSCs were isolated following a previously published method by our laboratory (Hegab et al., 2012b, 2012a, 2014; Paul et al., 2014). Briefly, airways were dissected, cleaned, and incubated in 16U/mL dispase for 30 min at room temperature. Tissues were then incubated in 0.5mg/mL DNase for another 30 min at room temperature. Epithelium was stripped and incubated in 0.1% Trypsin-EDTA for 30 min shaking at 37°C to generate a single cell suspension. Isolated cells were passed through a 40 μm strainer and plated for Air-Liquid Interface cultures.

Air-Liquid Interface Cultures

24-well 6.5mm transwells with 0.4 μm pore polyester membrane inserts were coated with collagen type I dissolved in cell culture grade water at a ratio of 1:10. 100 μl was added to each transwell and allowed to air dry. ABSCs were seeded at 100,000 cells per well directly onto collagen-coated transwells and allowed to grow in the submerged phase of culture for 4-5 days with 500 μL media in the basal chamber and 200 μL media in the apical chamber. ALI cultures were then established and cultured with only 500 μL media in the basal chamber, and cultures were harvested at varying time points for IF studies. Media was changed every other day and cultures were maintained at 37°C and 5% CO_2.

Tracheal Epithelial Cell Plus and Serum-Free Media

Human ABSCs/NHBEs were grown in TEC Plus media and TEC serum-free media during the submerged and ALI phases of culture, respectively. TEC base media is DMEM/Ham's F12 50/50 (Corning 15090CV). Table S1 indicates the media components and concentrations for TEC Plus and TEC serum-free media.

Cigarette Smoke *In Vitro* Treatments

A sterile chamber of 0.4 cu. ft. volume, with an attached vacuum pump, was used to generate and deliver CS. The ALI plates (without lids) were placed inside the chamber and exposed to the CS of a 1R3F research cigarette (University of Kentucky, Lexington, KY), which was attached to the vacuum chamber tube with a cigarette holder. The cigarette was burned 10% of its length and the CS was introduced into the chamber via suction pump. A previously optimized treatment of 3-min exposure/day was continued for 4 days.

SARS-CoV-2 infection

SARS-CoV-2, Isolate USA-WA1/2020, was obtained from Biodefense and Emerging Infectious (BEI) Resources of National Institute of Allergy and Infectious Diseases (NIAID). All the studies involving live virus were conducted in the UCLA BSL3 high-containment facility with appropriate institutional biosafety approvals. SARS-CoV-2 was passaged once in Vero-E6 cells and viral stocks were aliquoted and stored at −80°C. Virus titer was measured in Vero-E6 cells by $TCID_{50}$ assay.

ALI cultures on the apical chamber of transwell inserts were infected with SARS-CoV-2 viral inoculum (MOI of 0.1; 100 μl/well) prepared in ALI TEC media. The basal chamber of the transwell contained 500 μl of ALI media. For mock infection, ALI media (100 μl/well) alone was added. The inoculated plates were incubated for 2 hr at 37°C with 5% CO_2. At the end of incubation, the inoculum was removed from the apical chamber. At selected time points live cell images were obtained by bright field microscopy. Striking cytopathic effect (CPE) was observed in SARS-CoV-2 infected cells, indicating viral replication and associated cell injury. At 72 hours post infection (hpi), viral infection was examined by immunofluorescence (IF) analysis using a SARS-CoV antibody [BEI Resources: NR-10361 Polyclonal Anti-SARS Coronavirus (antiserum, Guinea Pig). SARS-CoV antigen was detected in the cytoplasm of the infected cells, revealing active viral infection.

Interferonβ-1 Drug Study

Once the ALI-SARS-CoV-2 infection system was established, we evaluated the effect of interferonβ-1 (200ng/mL) and remdesivir (10 μM), as a control. The ALI cultures in 24-well plates were pretreated with Interferonβ-1 for 1 hour, then SARS-CoV-2 inoculum (MOI 0.1) was added. DMSO vehicle treated cells, with or without viral infections, and with and without smoking exposure were included as controls. At 72 hpi, the cells were fixed and immunostained with Polyclonal Anti-SARS-CoV to assess viral genome replication (Figure 1C).

METHOD DETAILS

Immunocytochemistry, Confocal Imaging and Cell Counting

ALI cultures were fixed in 4% paraformaldehyde for 15 min followed by permeabilization with 0.5% Triton-X for 10 min. Cells were then blocked using serum-free protein block (Dako X090930) for one hour at room temperature and overnight for primary antibody incubation. After several washes of Tris-Buffered Saline and Tween-20 (TBST), secondary antibodies were incubated on samples for 1 hour in darkness, washed, and mounted using Vectashield hardest mounting medium with DAPI (Vector Labs H-1500). IF images were obtained using an LSM700 or LSM880 Zeiss confocal microscope and composite images generated using ImageJ. The list of antibodies used is provided in the Key Resources Table as part of STAR Methods. Cells were counted manually in a blinded fashion. Approximately equal numbers of cells (around 1,000 cells) were counted for each experimental group. All immunofluorescence images used for scoring cells consisted of a z series of optical sections captured on the Zeiss LSM 700 or 880 confocal microscopes.

Quantitative Polymerase Chain Reaction

RNA was isolated from the ALI cells with the RNeasy Mini Kit (QIAGEN 74104) following manufacturer's protocol and quantified using a NanoDrop Spectrophotometer (ThermoFisher). cDNA synthesis was performed using the TaqMan Reverse Transcription Reagents (ThermoFisher) or iScript cDNA Synthesis Kit (BioRad)s as indicated by the respective company. Quantitative real-time PCR for viral load was then performed with Cyber green using the primers in Table S2. Samples were run in triplicate and fold changes in expression were determined using the comparative ΔC_T method and GAPDH was used as an endogenous control. Quantitative real-time PCR for ACE2 was run with Taqman primer probes set Hs01085333_m1.

Viral Titer Measurement

The ALI cultures were infected with SARS-CoV-2 at MOI of 0.1, in transwell plates. Mock infected cells received only the media used for preparing the SARS-CoV-2 inoculum. After 1-hour incubation at 37°C with 5% CO_2, the inocula were removed. At each time point (days 1, 2 and 3), media from the basal chamber from mock and SARS-CoV-2 infected wells were collected and stored at −80°C. Viral production by infected ALI at each time point was measured by quantifying TCID50 (Median Tissue Culture Infectious Dose) as described (Gauger and Vincent, 2014). In brief, Vero-E6 cells were plated in 96-well plates at a density of 5 x10^3 cells/well. The next day, culture media samples collected from ALI at various time points were subjected to 10-fold serial dilutions (10^{-1} to 10^{-6}) and inoculated onto Vero-E6 cells. The cells were incubated at 37°C with 5% CO_2. After 72 hours, each inoculated well was examined for presence or absence of viral CPE and percent infected dilutions immediately above and immediately below 50% were determined. TCID50 was calculated based on the method of Reed and Muench.

Single Cell Library Generation and Sequencing

Single cells were obtained by incubating ALI cultures in 500ul Accumax for an hour and 15 min. Cells were then fixed in cold methanol per the Illumina protocol and frozen at −80°C. Cells were then rehydrated in ice cold PBS and RNase inhibitor per the Illumina protocol. Cells were captured using a 10X Chromium device (10X Genomics) and libraries prepared according to the Single Cell 3′ v2 or v3 Reagent Kits User Guide (10X Genomics, https://www.10xgenomics.com/products/single-cell-gene-expression/). Cellular suspensions were loaded on a Chromium Controller instrument (10X Genomics) to generate single-cell Gel Bead-In-EMulsions (GEMs). Reverse transcription (RT) was performed in a Veriti 96-well thermal cycler (ThermoFisher). After RT, GEMs were harvested, and the cDNA underwent size selection with SPRIselect Reagent Kit (Beckman Coulter). Indexed sequencing libraries were constructed using the Chromium Single-Cell 3′ Library Kit (10X Genomics) for enzymatic fragmentation, end-repair, A-tailing, adaptor ligation, ligation cleanup, sample index PCR, and PCR cleanup. Libraries QC was performed by the Agilent Technologies Bioanalyzer 2100 using the High Sensitivity DNA kit (Agilent Technologies, catalog# 5067-4626) and quantitated using the Universal Library Quantification Kit (Kapa Biosystems, catalog# KK4824. Sequencing libraries were loaded on a NovaSeq 3000 (Illumina).

Sequencing Data Analysis

Raw sequencing data were filtered by read quality, adaptor- and polyA-trimmed, and reads were aligned to a hybrid human hg38-SARS Covid2 transcriptome using the Cell Range software (10X Genomics) and the STAR aligner. Expression counts for each gene were collapsed and normalized to unique molecular identifiers to construct a cell by gene matrix for each library, filtered to keep cells with over 2000 transcripts and genes expressed in at least 0.05% of cells.

Data analysis was performed in R. Expression matrices were normalized by the total number of transcripts per cell in log space by dividing raw counts by the total number of transcripts per cell, then multiplying by 10,000. Two-dimensional visualization was obtained with the UMAP package. To identify major cell types in our normal integrated datasets, previously published lung epithelial cell type specific gene lists (Plasschaert et al., 2018) were used to create cell type-specific gene signatures, with cells assigned by maximal identity score. To identify differentially expressed genes between samples, we selected genes from every given pair of condition comparisons which satisfied an average expression difference of 33% either up or down in log normalized counts, filtered by a Bonferroni corrected $p < 0.01$. Gene ontology enrichments were determined using the Metascape tool (Zhou et al., 2019). For heatmap generation, the mean expression per condition was calculated and then per gene normalized to the maximal sample value.

QUANTIFICATION AND STATISTICAL ANALYSIS

The percentage of each cell population in each field was determined by dividing marker positive cells by the total number of nuclei. 2-way ANOVA was used to determine statistically significant effects of either smoking or virus on the cell populations. Unpaired t test was used to determine statistical significance of viral infection between no CS and CS groups. Kruskal-Wallis non-parametric ANOVA was used to compare nuclei counts across different drug treatments. Significance was defined as $p < 0.05$. Statistical details of experiments can be found in the Results section and Figure legends.